Tuning of the charge in octahedral ferric complexes based on pyridoxal-N-substituted thiosemicarbazone ligands

Tido, Eddy W. Yemeli; Faulmann, Christophe; Roswanda, Robby; Meetsma, Auke; van Koningsbruggen, Petra J.

Published in:
Dalton Transactions

DOI:
10.1039/b911114j

Publication date:
2010

Tuning of the charge in octahedral ferric complexes based on pyridoxal-N-substituted thiosemicarbazone ligands†

Eddy W. Yemeli Tido,[a] Christophe Faulmann,[b] Robby Roswanda,[a] Auke Meetsma[c] and Petra J. van Koningsbruggen*[a]

Received 5th June 2009, Accepted 22nd September 2009
First published as an Advance Article on the web 15th December 2009
DOI: 10.1039/b911114j

Four novel mononuclear coordination compounds namely: $[Fe(Hthpy)_2](SO_4)_{1/2}\cdot 3.5H_2O$ **1**, $[Fe(Hthpy)_2]NO_3\cdot 3H_2O$ **2**, $[Fe(H_2mthpy)_2](CH_3C_6H_4SO_3)_3\cdot CH_3CH_2OH$ **3** and $[Fe(Hethpy)(ethpy)]\cdot 8H_2O$ **4**, (H_2thpy = pyridoxalthiosemicarbazone, H_2mthpy = pyridoxal-4-methylthiosemicarbazone, H_2ethpy = pyridoxal-4-ethylthiosemicarbazone), were synthesized in the absence or presence of organic base, Et_3N and NH_3. Compounds **1** and **2** are monocationic, and were prepared using the singly deprotonated form of pyridoxalthiosemicarbazone. Both compounds crystallise in the monoclinic system, $C2/c$ and $P2_1/c$ space group for **1** and **2**, respectively. Complex **3** is tricationic, it is formed with neutral bis(ligand) complex and possesses an interesting 3D channel architecture, the unit cell is triclinic, $P\bar{1}$ space group. For complex **4**, the pH value plays an important role during its synthesis; **4** is neutral and crystallises with two inequivalent forms of the ligand: the singly and the doubly deprotonated chelate of H_2ethpy, the unit cell is monoclinic, $C2/c$ space group. Notably, in **1** and **4**, there is an attractive infinite three dimensional hydrogen bonding network in the crystal lattice. Magnetic measurements of **1** and **4** revealed that a rather steep spin transition from the low spin to high spin Fe(III) states occurs above 300 K in the first heating step. This transition is accompanied by the elimination of solvate molecules and thus, stabilizes the high spin form due to the breaking of hydrogen bonding networks; compared to **2** and **3**, which keep their low spin state up to 400 K.

Introduction

Thiosemicarbazones and their metal complexes continue to attract considerable interest because of their reported antineoplastic, antitumour, antiviral and antimalarial activity.[1–8] In addition, their Fe(III) complexes derivatives may exhibit unusual thermal magnetic behaviour.[9] The recent literature[1] shows that this general class of ligands exhibits a wide range of stereochemistries in complexation with transition metal ions; few of these metal compounds have been adequately investigated. A variety of functional groups have been attached to the thiosemicarbazone entity in order to modify the physical, chemical and/or biological properties of the resulting metal complexes.[10] The substitution includes among others: (i) changing the point of attachment of the thiosemicarbazone moiety in the parent aldehyde or ketone; (ii) substitution at the terminal N^4 position; and (iii) variation of the parent aldehyde or ketone. It is well known that depending on the appropriate coordination atoms (O, N, X, where X = N, O, S, Se), the ligand can bind to the connectors (metal ions) either in its neutral, monoanionic or dianionic form.[11,12] This also derives from the fact that in solution, thiosemicarbazone consists of an equilibrium mixture of thione and thiol tautomers. In this regard, our attention is directed to the design of pyridoxal semi-, thiosemi-, and isothiosemicarbazones, which can adopt the above-mentioned forms and is especially crucial to the preparation of desirable compound by selecting the suitable synthetic procedure.

However, to the best of our knowledge, no study has been devoted to such synthetic variations. Therefore, depending upon preparative conditions, especially the pH of the reaction medium, the complex unit can be neutral, monocationic, tricationic and even be monoanionic. Up to now, most investigations on metal pyridoxal-4R-thiosemicarbazone complexes have involved uncharged mono(ligand) and/or charged bis(ligand). So, data on the complexes containing neutral bisligand metal compounds is really lacking. It is worth noting that octahedral ferric complexes of pyridoxal-4R-thiosemicarbazone ligands (R = H, Ph) are (well) known to exhibit cooperative $S = 1/2 \leftrightarrow S = 5/2$ spin-crossover associated with thermal hysteresis loops,[13] whereas expectedly in a majority of other transition metal systems involving this ligand so far known, either the HS or the LS prevails.[11] In general, Fe(III) spin crossover behaviour is related to many factors such as; counter anion, solvate molecules, intermolecular interactions or hydrogen bonding network, which mediate the intercentre communication in the solid.[14–17] Recent work carried out on ferrous complexes bearing imidazole-type ligand evidenced that the spin state of the

[a]*Stratingh Institute for Chemistry, University of Groningen, Nijenborgh 4, 9747, AG, Groningen, The Netherlands. E-mail: p.j.van.koningsbruggen@rug.nl; Fax: +31 (0)-50-363 4315; Tel: +31 (0)-50-363 4363*
[b]*Laboratoire de Chimie de Coordination, LCC-CNRS UPR8241, 205 route de Narbonne, 31077, Toulouse, France*
[c]*Zernike Institute for Advanced Materials, University of Groningen, Nijenborgh 4, 9747, AG, Groningen, The Netherlands*

† Electronic supplementary information (ESI) available: IR, magnetic data and selected intra- and interatomic hydrogen bond distances. CCDC reference numbers 732214–732216 for **1**, **2** and **4** and 735943 for **3**. For ESI and crystallographic data in CIF or other electronic format see DOI: 10.1039/b911114j

metal center can also be tuned through the protonation state of the ligand,[18] as this may influence the ligand field strength about the metal ion. Considering these features, our report aims on varying the charge of the metal complex by essentially maintaining the same geometry around the central atom, and thereby, tuning the spin state of the metal ion. For this purpose, we designed and characterized four novel Fe(III) compounds where rather unprecedentedly both, the degree of deprotonation of the ligand and the charge of the metal complex vary; we also discussed and compared their magnetic properties.

Results and discussion

Synthesis

The pyridoxal-N-substituted thiosemicarbazone hydrochloride derivatives (Scheme 1) were prepared according to a procedure described in the literature[19] employing the condensation reaction of the corresponding thiosemicarbazide derivative and 3-hydroxy-5-(hydroxymethyl)-2-methyl-4-pyridinecarbaldehyde. Previously, these compounds have been prepared by refluxing the reaction mixture in ethanol.[13] The use of water as a reaction medium proves to be much more effective at generating the desired compounds in crystalline form but produces smaller yield and requires recrystallization.[20] Nevertheless, this type of Schiff-base, pyridoxal-N-substituted thiosemicarbazone hydrochloride salts are Brønsted–Lowry acids, and treatment with a mild base such as triethylamine is sufficient to afford the corresponding pyridoxal-N-substituted thiosemicarbazone monohydrate within 24 h in essentially quantitative yield (Scheme 1); (additional experiments showed that stronger bases such as NaOH, KOH were not suitable for this purpose). These ligands have been prepared previously, though in an entirely different manner.[21] As the resulting compounds are insoluble in non-protic solvents, the triethylammonium chloride ($Et_3N{\cdot}HCl$) formed can be easily removed by washing the residue with dichloromethane. Recrystallisation of the products from water–ethanol at room temperature afforded the products in pure, chloride-free form. Absence of chloride impurities was established in the first instance by a negative test reaction with aqueous $AgNO_3$ and then by elemental analysis.

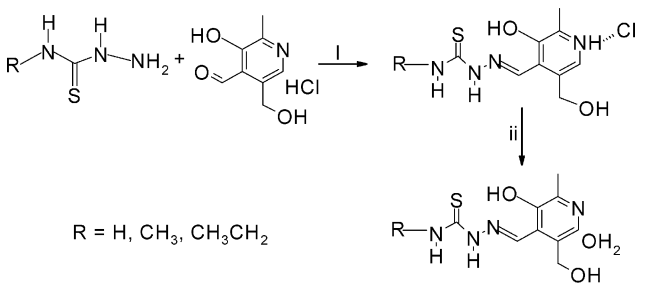

i = 4 h refluxing in EtOH; ii = $Et_3N + CH_2Cl_2$, overnight stirring.

Scheme 1 Synthesis of pyridoxal-N-substituted thiosemicarbazone monohydrate.

In DMSO-d_6, the ^{1}H NMR spectra undergo only minor changes on conversion of the pyridoxal-N-substituted thiosemicarbazone hydrochloride form to the monohydrate derivatives. However, the IR spectra of the hydrochloride free form (ESI Fig. S1b†) clearly differ from those with hydrochloride (ESI Fig. S1a†). The hydrochloride form contains weak/medium absorptions in the range 2700–2850 cm^{-1}, which have been assigned to N–H–Cl vibrations. In the monohydrate these vibrational bands are no longer observed, providing further evidence that chloride is no longer present. Although OH and NH units are still present in the hydrochloride free form, its interaction with the H_2O molecules appears to have changed considerably, accordingly, most of the bands in the 2500–3500 cm^{-1} region of the IR spectrum have disappeared.

This class of ligands can be complexed to transition metal ions by several routes and in three different forms. Metallation with alkali reagents can be accomplished using NH_3 or Et_3N to generate the desired salts. Several structurally characterized examples have already been reported.[22–27] Reaction of pyridoxal-N-substituted thiosemicarbazone hydrochloride and iron(III) sulfate pentahydrate in methanolic solution produces the monoanionic coordination complex with two monodeprotonated ligands. The same charge of the metal complex is obtained with its iron(III) chloride salts but the ligated mono(ligand) is of its neutral form.[28] On the other hand, the addition of concentrated ammonia at room temperature to a solution containing pyridoxal-N-substituted thiosemicarbazone hydrochloride on constant stirring leads to the neutralisation of HCl and the deprotonation of the chelate in solution. Thus, dropwise addition of a solution containing the appropriate iron(III) salt results in dark green solution (the pH of the reaction mixture should not be below 10.40 or exceed 10.70), followed by filtration and slow evaporation at room temperature, gives the analytically pure paramagnetic complex in good yield. If an excess of ammonia solution is added, no further deprotonation is observed. However, the metal compound is neutral and the ligand binds to the metal ion in two inequivalent forms: the singly and the doubly deprotonated form, suggesting the formation of a very stable compound.

Once HCl has been removed, the ligands can be used directly with suitable metal precursors such as iron(III) nitrate nanohydrate or iron(III) *p*-toluenesulfonate hexahydrate in metathesis reactions in water or ethanol, respectively. In the first case of complexation, the charge of metal complex is +1 and the two ligated ligands are singly deprotonated while in the second case, the resulting charge is +3 and the two ligated ligands are of its uncharged form. These results demonstrate that factors such as the nature of the iron(III) salt, pH and as well as the substituent at the terminal N^4 position of the thiosemicarbazone moiety play an important role during the synthesis.

Description of structures

X-Ray structural analysis of **1** and **2** reveals that they are monoclinic in unit cell, of different space group and constructed from a unique 1D basic subunit ($[Fe(Hthpy)_2]^+$). The asymmetric unit of **1** consists of eight moieties: a cationic Fe-complex, a half of a sulfate anion, with S at special position: ·2· (two fold axis parallel the *b*-axis), and six solvate water molecules, of which five are partly occupied. Whereas, that of **2** consists of five moieties: a cationic Fe-complex, a nitrate anion, and three water solvate molecules, with no atom setting at special position. Though complex **4** is isomorphic to **1**, it is not built up from the same

subunits. Its asymmetric unit contains nine moieties: a neutral Fe-complex and eight water solvate molecules. In each case, these entities are linked by hydrogen bonds,[29–31] forming an infinite three-dimensional network along the crystal axes. However, **3** crystallises in the triclinic space group $P\bar{1}$. The asymmetric unit contains five moieties: a tricationic Fe-complex, three tosylate anions and one ethanol solvate molecule, with no atom setting at special position. The moieties are linked by hydrogen bonds,[29–31] forming an infinite one-dimensional chain along the base vector [001]. The molecular structures and the packing arrangement are illustrated in Fig. 1–4. Relevant bond lengths and angles are given in the Electronic Supplementary Information.

In these four compounds, the Fe(III) atom is coordinated by two tridentate O,N,S-ligands, with the formation of a distorted $FeS_2N_2O_2$ octahedron. The donor atoms are located in mutually normal planes, the S and O atoms being at the cis-positions and N at the *trans*-positions. Particularly, the binding of the ligand involving the formation of two metallocycles: a five-membered

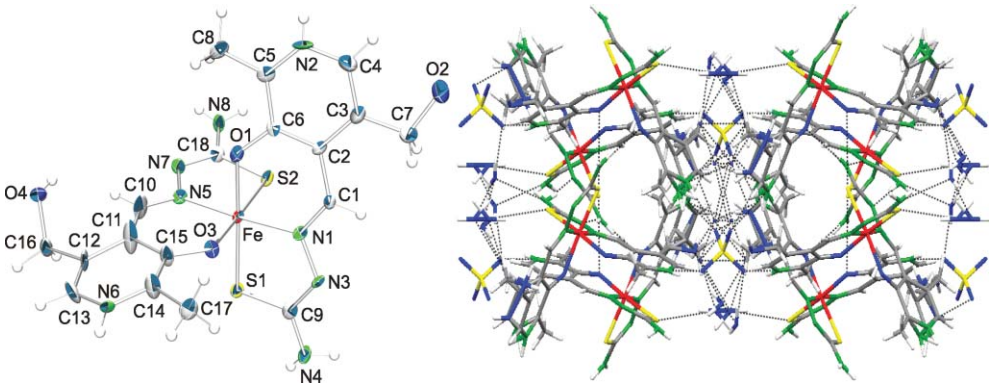

Fig. 1 X-Ray structure of **1** showing the coordination environment (thermal ellipsoids at the 70% probability level). Water molecules, and sulfate anions are omitted for clarity and view down the *c* axis, illustrating the molecular packing and hydrogen-bonding scheme.

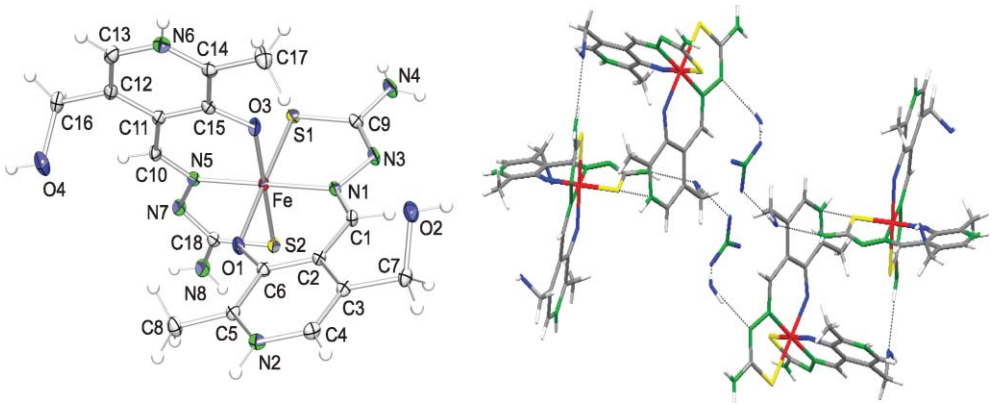

Fig. 2 X-Ray structure of **2** showing the coordination environment (thermal ellipsoids at the 50% probability level). Water molecules, and nitrate anions are omitted for clarity and view down the *a* axis, illustrating the molecular packing and hydrogen-bonding scheme.

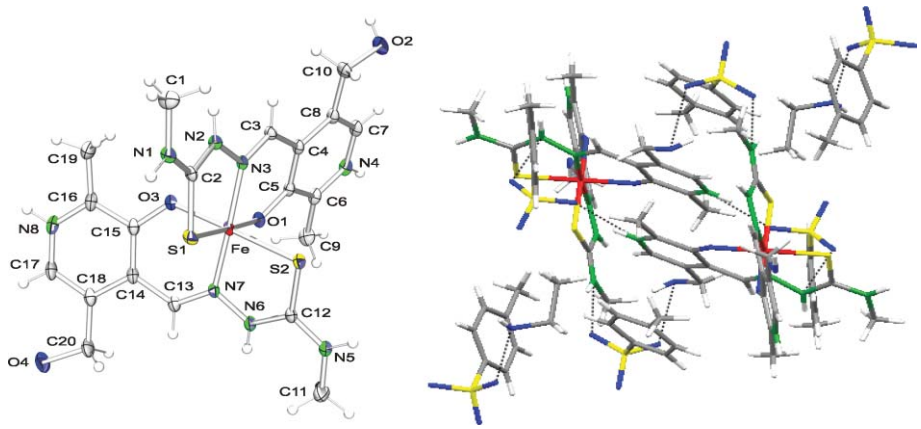

Fig. 3 X-Ray structure of **3** showing the coordination environment (thermal ellipsoids at the 20% probability level). Ethanol molecule, and *p*-toluenesulfonate anions are omitted for clarity and view down the *a* axis, illustrating the molecular packing and hydrogen-bonding scheme.

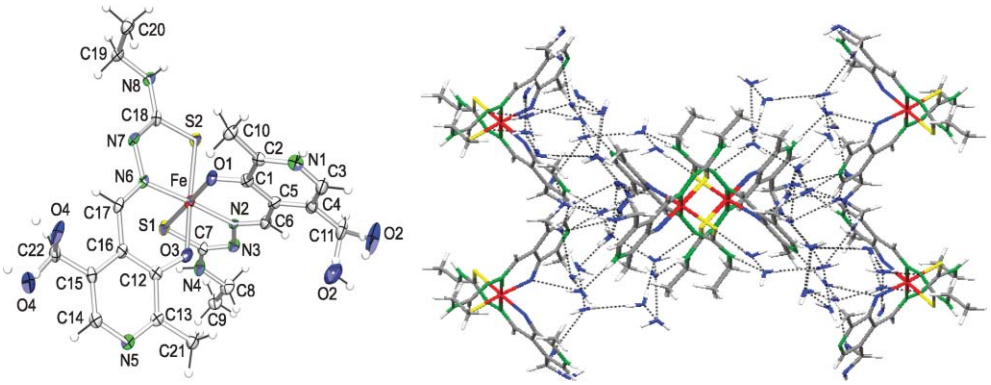

Fig. 4 X-Ray structure of **4** showing the coordination environment (thermal ellipsoids at the 50% probability level). Water molecules are omitted for clarity and view down the *a* axis, illustrating the molecular packing and hydrogen-bonding scheme.

thiosemicarbazide S,N-chelate ring together with a six-membered pyridoxilydene N,O-chelate ring, appears to be associated with a severe deviation from planarity of the iron-ligand framework. The angle between the least-squares planes through these five-membered and six-membered rings is approximately 6.83(5)°. In **3**, pyridoxal-4-methylthiosemicarbazone appears to be of its neutral zwitterionic form, *i.e.* it is deprotonated at the phenolic oxygen atoms O1, O3 whereas it is protonated at the pyridine N4, N8 and the hydrazinic N2, N6 nitrogen. Protonation of N4, N8 is evident from the value of the C6–N4–C7 and C16–N8–C17 pyridyl angle of 124.6(5)° and 124.8(4)°, which have significantly increased with respect to the C–N–C angle of about 120° that could be expected for a non-protonated pyridyl-N. In addition, protonation of N2, N6 is in line with the ligand being of the thione form, *i.e.* having typical short C2–S1, C12–S2 distances of 1.718(4) and 1.713(4) Å and adjacent carbon–nitrogen bond lengths which are typical for a single bond (C2–N2 = 1.338(4) Å, C12–N6 = 1.332(5) Å). These bond distances are in agreement with the literature values.[21,22] In **1** and **2**, pyridoxalthiosemicarbazone binds in its monoanionic form to the metal ion, *i.e.* the nitrogen of the pyridine ring bears a proton whereas that of the hydrazinic nitrogen does not possess any hydrogen; several additional structural features to characterize the ligand form of **1** and **2** can be obtained from the bond distances and angles given in the ESI material. In contrast to **1**, **2** and **3** whose ligands are equally bonded to iron, complex **4** is formed with two inequivalent forms of the ligand. Both ligands are obtained by sequentially deprotonating neutral pyridoxal-4-ethylthiosemicarbazone. The singly deprotonated ligand ($Hethpy^-$) possesses a hydrogen atom bound to the N1 nitrogen atom, whereas no such hydrogen atom is found at the N5 position of the doubly deprotonated form ($ethpy^{2-}$). Thus, it is easily seen from the angle about the pyridyl nitrogen, which is 118.3(4)° for the dianionic form and of 123.0(5)° for the monoanionic ligand. Specific structural differences between the singly and doubly deprotonated ligands, as well as differences in the manner in which each binds to the iron center, are illustrated in Fig. 4. X-Ray structural data of Fe(III) bis-ligand compounds of the dianion of R-salicylaldehyde thiosemicarbazone reveal that the Fe–S, Fe–O and Fe–N distances typically are of the order of 2.44 Å, 1.96 Å and 2.12 Å for high spin Fe(III), respectively, whereas these are 2.23 Å, 1.94 Å and 1.96 Å for low spin Fe(III), respectively.[32] Comparison with these iron ligand bond lengths indicates that the Fe(III) ion is in the low spin state in the studied complexes. Fig. 1–4 illustrate the molecular packing and hydrogen bonding scheme in the unit cell along the three-dimensional axis. The molecules of compounds **1–4** are held together by N–H–O, N–H–S, O–H–S, O–H–N, and O–H–O hydrogen bonds. A summary of the hydrogen-bond dimensions is given in the ESI, Table S1.†

Thermogravimetric analysis

The observed percentage weight loss corresponding to the first inflexion in the thermograms of both compounds were compared (Fig. 5a and 5b) with those calculated on the basis of possible decomposition of the expelled moieties. In the present study, the TGA profile consists of two well defined stages. Upon heating between 357 and 403 K, the complexes liberate solvate molecules. The theoretical weight loss for this step is 9.76% for **1** and 19.63% for **4**. The experimental weight losses are 8.60% and 17.73% for **1** and **4**, respectively, which are very close to the theoretical values. Here, the compounds are completely devoid of lattice solvent molecules. Then the curves showed a straight line, which did not change even on heating up to 497 K, indicating that there is no further change in weight. Finally, the last step of decomposition starts from around 497 K and continues even beyond 523 K involving deterioration of the compounds.

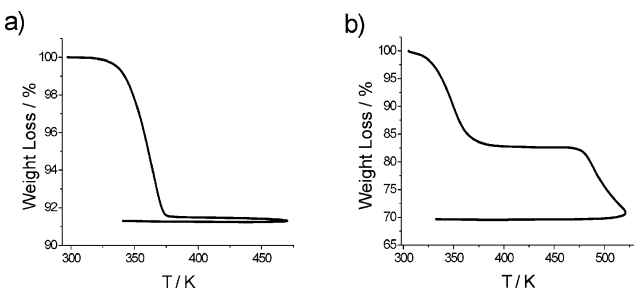

Fig. 5 TGA curve of: (a) $[Fe(Hthpy)_2](SO_4)_{0.5}\cdot 3.5H_2O$ and (b) $[Fe(Hethpy)(ethpy)]\cdot 8H_2O$.

Magnetic properties

Fig. 6b shows the thermal variation (heating and cooling modes) of the effective magnetic moment, μ_{eff} of **4**. From 2–300 K, a roughly

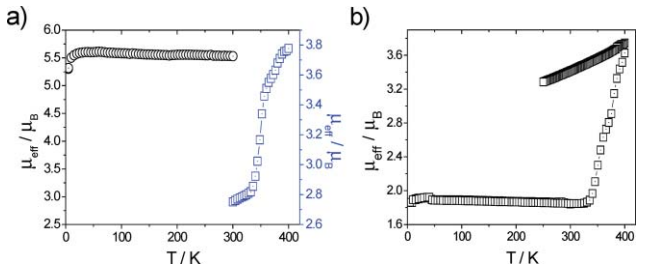

Fig. 6 Magnetic behaviour of: (a) $[Fe(Hthpy)_2](SO_4)_{0.5}\cdot 3.5H_2O$ in the form of μ_{eff} *vs.* T plots. The sample was first warmed from 300 to 400 K (□) before being placed in an oven at 497 K for 2 h. After removal of solvent molecules, μ_{eff} was then measured from 5 to 300 K (○), and (b) $[Fe(Hethpy)(ethpy)]\cdot 8H_2O$ in the form of μ_{eff} *vs.* T plots. The sample was warmed from 2 to 400 K (□) and then cooled from 400 to 250 K (□), at a rate of 2 K min^{-1}.

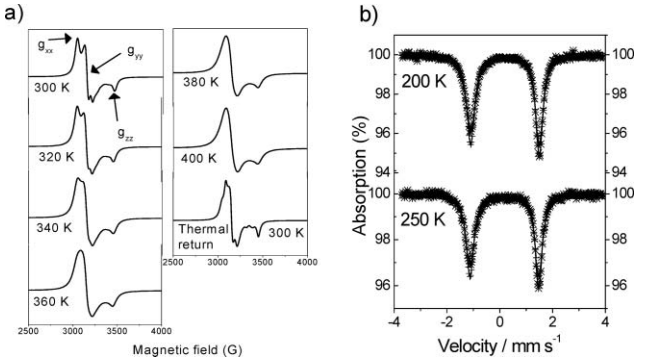

Fig. 7 (a) Temperature dependence X-band spectrum above RT with microwave frequency 9.510743 GHz and (b) ^{57}Fe Mössbauer spectra at 200 and 250 K of $[Fe(H_2mthpy)_2](CH_3C_6H_4SO_3)_3\cdot CH_3CH_2OH$.

constant μ_{eff} equal to $1.85\mu_B$ is observed. This value is in agreement with the presence of 100% of the Fe(III) cations in the LS state, as was already deduced from X-ray diffraction. Upon heating above 300 K, μ_{eff} increases to reach a value of $3.87\mu_B$ at 400 K. It is somewhat smaller than the expected "spin-only" value for one Fe(III) HS per formula unit. On cooling the sample below 400 K, a constant μ_{eff} value of ~$3.6\mu_B$ is obtained, which is close to that observed at 400 K. Clearly, **4** is changing its configuration from the LS state to the HS state during dehydration. TGA measurements show weight loss in this temperature range. Thus, after annealing the sample in the TGA up to 497 K (in order to get rid of water molecules), the anhydrous material was then placed in the squid magnetometer. The recorded temperature dependence of the effective magnetic moment (ESI, Fig. S4†) yielded a constant value of $5.52\mu_B$ that did not change during the warming and cooling runs (100–220 K), respectively. As a consequence, complex **4** is HS after being transformed completely to an anhydrous material ([Fe(Hethpy)(ethpy)]). Complex **1** exhibits similar behaviour (Fig. 6a), with the only exception that below room temperature, the effective magnetic moment is slightly higher than the spin only value expected for Fe(III) low spin (ESI, Fig. S3a†). In contrast to **1** and **4**, compound **2** is low spin; even when heating from 200 to 400 K, the effective magnetic moment remains constant and equal to: $\mu_{eff} = 2.06\mu_B$ (ESI, Fig. S2a†). Crystallographic studies at both 100 K and room temperature revealed the same crystal information. On the other hand, variable X-band EPR spectra above room temperature (ESI, Fig. S2b†) does not show any signal related to the high-spin form.

The solid-state X-band EPR spectrum recorded on a polycrystalline sample at 300 K (Fig. 7a) for **3**, shows a typical spectrum for low spin iron(III) ion in a rhombic symmetry with $g_{xx} = 2.23$, $g_{yy} = 2.15$, and $g_{zz} = 1.96$. Similar signals were reported earlier for the Fe(III) center in a spin equilibrium system.[33,34] The temperature dependence of the EPR signal observed above room temperature is strongly influenced by the temperature, which affects not only its intensity, but also its shape. Upon heating, the rhombic signal slowly changes to an axial anisotropic signal from 360 to 400 K, with $g_{\perp} = 2.15$ and $g_{\parallel} = 1.96$ and hence is typical for LS iron(III) center.[35] A rapid cooling down to 300 K experiment has been carried out with the objective to determine whether the compound was affected during heating. On performing this experiment, it appears that the spectrum recovered its anisotropic rhombic symmetry but with less intense g_{xx} signal.

^{57}Fe Mössbauer spectra of **3** recorded at 200 and 250 K consist of a single asymmetric quadrupole-split doublet as shown in Fig. 7b. The spectra were least-squares fitted with Lorentzian lines and the resulting isomer shift (IS) and quadrupole splitting parameters (ΔE_Q) are listed in Table 2. The magnitudes of IS and ΔE_Q are comparable to those observed for well characterized pure $S = \frac{1}{2}$ spin systems. In fact, LS iron(III) compounds have IS values in the range of 0.05–0.20 mm s^{-1} and relatively large ΔE_Q values of 1.9–3.0 mm s^{-1}.[36] This conclusion is supported by the effective magnetic moment (ESI, Fig. S3b†) and the EPR spectra recorded at/around the same temperatures.

Comparative study

The above results give compelling evidence of the role played by solvent molecules in the magnetic properties of the different complexes. It is clear that the magnetism of these salts is very sensitive to their solvate molecules and in other cases to the counterion, which is able to form hydrogen bonds. For instance, in a monocationic compound like **1** and **2**, where the ligand substitution and its degree of deprotonation are identical, their magnetic behaviour is completely different. **1** is showing an abrupt transition upon release of its co-crystallized water molecules, whereas **2** remains in the LS state even after losing its water molecules. Consequently, the variation of anion from SO_4^{2-} to NO_3^- associated with this cationic spin crossover system, result to the extent that the SCO behaviour is no longer observed. The influence of the anion for instance was noted for salts of $[Co(terpy)_2]^{2+}$[37] and for iron(II) in salts of $[Fe(paptH)_2]^{2+}$[38] and of $[Fe(pic)_3]^{2+}$.[39] If we replace the substituent at the terminal N^4 position of the thiosemicarbazone moiety by a methyl group and change the size of the counterion (from sulfate and nitrate anions to tosylate anion), we obtained a tricationic complex. As expected, although changes occurred on the lattice phonon distribution resulting from different crystal packing geometry and strength of the intermolecular forces, the iron(III) center is LS. Hence, modification does not bring about major fundamental changes in the nature of the transition or on the ligand field strength. On the order hand, in a neutral species like **4**, where the ligand is bound to the metal ion in two inequivalent forms, the transition occurs upon release of water molecules and breaking of the hydrogen bonding interactions. This phenomenon is irreversible and probably modifies completely the crystal lattice stacking

interactions. There are many other similar examples in the literature.[40–42] Whatever the rationale for the effects, it is clear that the magnetic properties of the four compounds are the same up till room temperature before behaving differently above room temperature upon release of their molecules of solvents.

Conclusions

A new family of octahedral ferric complexes based on pyridoxal-N-substituted thiosemicarbazone, including two monocationic complexes $[Fe(Hthpy)_2](SO_4)_{1/2}\cdot 3.5H_2O$ **1**, $[Fe(Hthpy)_2]NO_3\cdot 3H_2O$ **2**, one tricationic complex, $[Fe(H_2mthpy)_2](CH_3C_6H_4SO_3)_3\cdot CH_3CH_2OH$ **3**, and a neutral complex, $[Fe(Hethpy)(ethpy)]\cdot 8H_2O$ **4**, has been characterized and extensively investigated. The coordination chemistry of iron(III) so far reported reveals that this ligand system yields stable Fe(III) complexes of the uncharged monoligand and/or charged bisligands metal compound.[1] Within each degree of deprotonation, the ligands which afford SCO are further limited because the ligand field in a SCO compound should be close to the crossover point of the Tanabe–Sugano diagram.[43] In fact, the ligand environments which induce SCO are limited to $FeO_2N_2S_2$ octahedron. Therefore, it should be stressed that the present pyridoxal attached to three thiosemicarbazide groups provides an ONS donor set able to bind the central atom in a versatile form and thus stabilize a remarkable variety of charge of the iron(III) complex, as described in this study. Among the materials in this family, $[Fe(Hthpy)_2](SO_4)_{1/2}\cdot 3.5H_2O$ **1** and $[Fe(Hethpy)(ethpy)]\cdot 8H_2O$ **4** assume appealing infinite three dimensional hydrogen bonding network in their crystal lattice. The degree of deprotonation and the substituent effect of the methyl and ethyl groups at the terminal thiosemicarbazone chain allow fine-tuning of the charge of metal complex and SCO behaviour of this type of molecular system.

Experimental

Materials

Pyridoxal hydrochloride (99%), iron(III) *p*-toluenesulfonate ($Fe(CH_3C_6H_4SO_3)_3\cdot 6H_2O$) and iron(III) sulfate pentahydrate ($Fe_2(SO_4)_3\cdot 5H_2O$) have been purchased from Aldrich, whereas thiosemicarbazide (99%), 4-methyl-3-thiosemicarbazide (97%), 4-ethyl-3-thiosemicarbazide (97%), and iron(III) nitrate nanohydrate ($Fe(NO_3)_3\cdot 9H_2O$) have been purchased from Acros. All chemicals were used without further purification.

Physical measurements

Infrared spectra were recorded as KBr pellets in the 4000–400 cm^{-1} range on an Interspec 200-X FT-IR spectrometer. Routine EI+ spectra were measured with the MS route JMS-600H sector mass spectrometer (JEOL). ^1H NMR spectra were recorded in DMSO-d_6 with a Varian VXR- 300 spectrometers with TMS as standard (s, singlet; d, doublet; t, triplet; m, multiplet; s, br, singlet, broad). Elemental analysis was carried out at the Microanalytical Department of the University of Groningen, using the Euro EA Elemental Analyzer from the EuroVector Instrument and Software Company. Variable-temperature, solid state magnetic susceptibility data from 2 to 400 K were collected on a Quantum Design MPMS SQUID magnetometer equipped with a 7 T magnet. Diamagnetic corrections were applied to the observed paramagnetic susceptibilities using Pascal's constants.

The EPR measurements were performed in the range 293–420 K with an X-band Bruker ESP 300e spectrometer equipped with a variable temperature accessory from Oxford Instruments. The crystals are mounted on a small Perspex sample holder to allow their orientation with respect to the magnetic field. The microwave frequency is measured with a Systron Donner frequency counter.

Mössbauer experiments

The variable temperature ^{57}Fe Mössbauer measurements were carried out by means of a conventional constant-acceleration spectrometer with a 50 mCi $^{57}Co(Rh)$ source on *ca.* 100 mg powder sample enclosed in a 12 mm diameter cylindrical plastic sample holder. The samples were cooled down in a custom-designed, liquid helium flow-type cryostat. A least-squares computer program was used to fit the Mössbauer parameters and to determine the standard deviations of statistical origin.[44] The isomer shift values are given with respect to metallic iron at room temperature.

Thermal analysis

Thermogravimetric measurements were carried out using a Perkin-Elmer TGA7 apparatus in the temperature range 25–250 °C under inert atmosphere (N_2) with 5 °C min^{-1} heating rate.

X-Ray crystallography and structure solution

Crystallographic data and numerical details on data collection and refinement for compounds **1–4** are summarized in Table 1. All data collections were performed on a Bruker SMART APEX CCD diffractometer (Platform with full three-circle goniometer), equipped with a 4K CCD detector set 60.0 mm from the crystal. Intensity measurements were performed using graphite monochromated Mo-Kα radiation from a sealed ceramic diffraction tube (SIEMENS). Suitable crystals were mounted on top of a glass fiber, aligned and cooled to 100(1) K using the Bruker KRYOFLEX low-temperature device. Data integration and global cell refinement was performed with the program SAINT,[45] intensity data were corrected for Lorentz and polarisation effects, scale variation, for decay and absorption: a multi-scan absorption correction was applied, based on the intensities of symmetry-related reflections measured at different angular settings (SADABS),[46] and reduced to F_o^2. The program suite SAINTPLUS was used for space group determination (XPREP).[45]

All structures were solved by direct methods using the program SIR2004,[47] Patterson methods and extension of the model was accomplished by direct methods applied to difference structure factors using the program DIRDIF.[48,49] All non hydrogen atoms were refined anisotropically. Hydrogen atoms were refined using the riding model.

The positional and anisotropic displacement parameters for the non-hydrogen atoms and isotropic displacement parameters for hydrogen atoms were refined on F^2 with full-matrix least-squares procedures minimizing the function $Q = \sum_h[w(|(F_o^2) - k(F_c^2)|)^2]$, where $w = 1/[\sigma^2(F_o^2) + (aP)^2 + bP]$, $P = [\max(F_o^2,0) + 2F_c^2]/3$, F_o and F_c are the observed and calculated structure factor amplitudes. Neutral atom scattering factors and anomalous dispersion corrections were taken from International Tables for

Table 1 Crystallographic data and structure refinement results for **1**, **2**, **3** and **4**

Compound	**1**	**2**	**3**	**4**
Formula	$C_{18}H_{29}FeN_8O_{9.5}S_{2.5}$	$C_{18}H_{28}$ $FeN_9O_{10}S_2$	$C_{43}H_{55}$ $FeN_8O_{14}S_5$	$C_{22}H_{45}$ $FeN_8O_{12}S_2$
Formula weight/g mol^{-1}	645.49	650.45	1124.10	733.62
Crystal system	Monoclinic	Monoclinic	Triclinic	Monoclinic
Space group	$C2/c$	$P2_1/c$	$P\bar{1}$	$C2/c$
Crystal colour	Dark brown	Dark red	Dark brown	Dark green
Crystal description	Platelet-shaped	Block	Platelet	Platelet-shaped
Crystal dimensions/mm	$0.39 \times 0.27 \times 0.10$	$0.47 \times 0.39 \times 0.28$	$0.47 \times 0.34 \times 0.17$	$0.47 \times 0.41 \times 0.07$
a/Å	27.416(2)	9.3807(6)	12.7197(4)	24.778(4)
b/Å	12.2927(8)	19.045(1)	14.0994(4)	11.6118(19)
c/Å	17.230(1)	15.885(1)	15.8183(4)	25.799(4)
α/°	106.167(1)	107.057(1)	95.1230(10)	116.310(2)
β/°	—	—	113.2920(10)	—
γ/°	—	—	92.9670(10)	—
V/Å^3	5577.2(6)	2713.1(3)	2583.47(13)	6653.9(18)
Z	8	4	2	8
ρ_{calcd}/g cm^{-3}	1.537	1.592	1.445	1.465
T/K	100(1)	100(1)	293(2)	100(1)
λ/Å	0.71073	0.71073	0.71073	0.71073
μ/cm^{-1}	7.9	7.78	5.64	6.47
F(000)	2680	1348	1174	3096
Total data	21 093	24 468	100 918	25 391
Unique data	5471	6727	11037	6762
R_{int}	0.0553	0.0225	0.0347	0.0614
$R(F)^a$	0.0903	0.0302	0.0574	0.0709
w$R(F^2)^b$	0.2056	0.0745	0.1623	0.1847
GOF on F^2	1.290	1.060	1.095	1.097
$\Delta_\rho$max, $\Delta_\rho$min/e Å^{-3}	0.8, –0.6(1)	0.44, –0.27(6)	1.139, –1.127	0.91, –0.57(11)

^{a} $R(F) = \sum(\|F_o\| - \|F_c\|)/\sum|F_o|$ for $F_o > 4.0\sigma(F_o)$ for observed reflections. ^{b} $wR(F^2) = [\sum[w(F_o^2 - F_c^2)^2]/\sum[w(F_o^2)^2]]^{1/2}$ for all data.

Table 2 ^{57}Fe Mössbauer spectral parameters of $[Fe(H_2mthpy)_2](CH_3C_6H_4SO_3)_3 \cdot CH_3CH_2OH$ at 200 and 250 K, with ΔE_Q the quadrupole splitting and IS the isomer shift (relative to metallic iron)

	IS/mm s^{-1}	ΔE_Q/mm s^{-1}	$\Gamma/2$/mm s^{-1}	LS fraction (%)
250 K	0.18(37) $\chi^2 = 1.46$	2.60(74)	0.18(61)	100
200 K	0.19(25) $\chi^2 = 2.57$	2.59(51)	0.18(42)	100

Crystallography.[50,51] All refinement calculations and graphics were performed on a HP XW6200 (Intel XEON 3.2 Ghz)/Debian-Linux computer at the University of Groningen with the program packages SHELXL [33,52] (least-square refinements), a locally modified version of the program PLUTO[53,54] (preparation of illustrations) and PLATON [55,56] package (checking the final results for missed symmetry with the MISSYM option, solvent accessible voids with the SOLV option, calculation of geometric data and the ORTEP [55,56] illustrations).

Synthesis

Pyridoxal thiosemicarbazone hydrochloride (H_2thpy·HCl). H_2thpy·HCl has been prepared according to a procedure described in literature.[21] Yield: (12.83 g, 94.5%); mp 212 °C (from EtOH). (Found: C 39.08, H 4.74, N 20.07, S 11.60. Calcd for $C_9H_{13}N_4O_2S$·HCl: C 39.06, H 4.73, N 20.25, S 11.58%). H_2thpy·HCl is soluble in water, ethanol, but scarcely dissolves in acetone, chloroform and methanol, even at elevated temperatures. ν_{max} (KBr)/cm^{-1} 3294 (NH), 3164 (OH), 2773 (NH^+), 1641 (CN), 1572 (py), 1369 (OH), 1256 (NN), 1185 (CN) and 1017 (CS). δ_H(300 MHz; DMSO-d_6; Me_4Si) 10.46 (1 H, br s, NH-3), 9.29 (1 H, br s, OH py), 8.56 (1 H, s, HC=N), 8.33–8.10 (2 H, br s, NH_2), 7.96 (1 H, s, py), 5.26 (1 H, t, OH), 4.87 (2 H, s, py CH_2O) and 1.74 (3 H, s, CH_3 py). m/z (EI) 239.8 ($M^+ = HCl \cdot C_9H_{13}N_4O_2S$ requires 240), 196 (7%), 165 (100), 150 (41), 119 (11), 77 (22) and 60 (17).

Pyridoxal thiosemicarbazone monohydrate (H_2thpy·H_2O). Under an inert atmosphere of dry nitrogen, a mixture of pyridoxal hydrochloride (0.049 mol) and thiosemicarbazide (0.049 mol) in ethanol on constant stirring was refluxed at 60 °C for 4 h during which time the reaction mixture turned into a yellow solid. The solid was washed with diethyl ether (3 × 30 mL) and dried under vacuum for 24 h to give pyridoxalthiosemicarbazone hydrochloride (H_2thpy·HCl). Subsequently, a mixture of H_2thpy·HCl (0.0454 mol) and triethylamine (0.0089 mol) in dichloromethane (200 mL) was stirred at RT for 24 h under an inert atmosphere of dry nitrogen. The resulting yellow precipitate was filtered off under vacuum, washed with dichloromethane (3 × 20 mL) and recrystallized from water–ethanol solution to give the final product (10.87 g, 92.8%); mp 226 °C (from EtOH/H_2O). (Found: C 43.49, H 5.06, N 21.43, S 12.97. Calcd for $C_9H_{12}N_4O_2S \cdot H_2O$: C 42.01, H 5.09, N 21.78, S 12.46%). H_2thpy·H_2O is soluble in DMSO, DMF but not in water, ethanol and methanol, even at elevated temperatures. ν_{max} (KBr)/cm^{-1} 1616 (CN), 1520 (py), 1381 (OH), 1100 (NN) and 1035 (CS). δ_H(300 MHz; DMSO-d_6; Me_4Si) 11.60 (1 H, br s, NH-3), 9.65 (1 H, br s, OH py), 8.57 (2 H, s, py CHN + NH-4), 7.99 (1 H, s, py), 5.25 (1 H, s, OH), 4.57 (2 H, s, py CH_2O) and 1.76 (3 H, s, CH_3 py). m/z (EI) 239.7 ($M^+ = H_2O \cdot C_9H_{13}N_4O_2S$ requires 240), 206 (7%), 165 (100), 150 (41), 120 (12), 77 (23) and 60 (16).

Pyridoxal-4-methylthiosemicarbazone monohydrate (H_2mthpy·H_2O). In a typical procedure, a mixture of pyridoxal hydrochloride (0.098 mol) and triethylamine (0.0089 mol) in dichloromethane (200 mL) was stirred at RT for 24 h under an inert atmosphere of dry nitrogen. The triethylamine hydrochloride salt formed during this reaction is soluble while the solid obtained was filtered off, washed with dichloromethane (3 ×15 mL) and recrystallized from a water–acetone solution and dried under vacuum for 24 h to give pyridoxal of its free form. Thereafter, a mixture containing pyridoxal free hydrochloride (0.061 mol) and 4-methyl-3-thiosemicarbazide (0.061 mol) in ethanol solution on constant stirring was refluxed at 60 °C for about 4 h during which time the reaction mixture turned into a yellow solid. The solid was washed with diethyl ether (3 × 30 mL) and dried under vacuum for 24 h to give pyridoxal-4-methylthiosemicarbazone monohydrate (H_2mthpy·H_2O) (10.15 g, 68.2%); mp 228 °C (from EtOH). (Found: C 44.60, H 5.85, N 20.58, S 12.07. Calcd for $C_{10}H_{14}N_4O_2S$·H_2O: C 44.11, H 5.92, N 20.57, S 11.77%). H_2mthpy·H_2O is soluble in DMSO, DMF and insoluble in water, ethanol and acetone, even at elevated temperatures. ν_{max} (KBr)/cm^{-1} 3375 (NH), 2953 and 2919 (CH), 2849 (NH^+), 1629 (CN), 1550 (py), 1385 (OH), 1260 (NN) and 1044 (CS). δ_H(300 MHz; DMSO-d_6; Me_4Si) 11.60 (1 H, br s, NH-2), 9.93 (1 H, br s, OH py), 8.56 (2 H, s, py CHN + NH-4), 7.98 (1 H, s, py), 5.26 (1 H, t, OH), 4.56 (2 H, d, py CH_2O), 2.99 (3 H, s, CH_3N) and 1.75 (3 H, s, CH_3 py). *m/z* (EI) 253.8 ($M^+ = H_2O·C_{10}H_{14}N_4O_2S$ requires 254), 180 (17%), 165 (100), 150 (26), 105 (21), 74 (39) and 57 (37).

Pyridoxal 4-ethylthiosemicarbazone hydrochloride (H_2ethpy·HCl). H_2ethpy·HCl has been prepared according to a procedure described in literature.[21] Yield: (13.41 g, 89.6%); mp 214 °C (from EtOH). (Found: C 43.23, H 5.73, N 18.11, S 10.43. Calcd for $C_{11}H_{16}N_4O_2S$·HCl: C 43.35, H 5.62, N 18.38, S 10.52%). H_2ethpy·HCl is soluble in water, ethanol, but scarcely dissolves in acetone, chloroform and methanol, even at elevated temperatures. ν_{max} (KBr)/cm^{-1} 3262 (NH), 3148 (OH), 2923 and 2852 (CH), 2759 (NH^+), 1622 (CN), 1581 (py), 1328 (OH), 1258 (NN), 1196 CN) and 1017 (CS). δ_H(300 MHz; DMSO-d_6; Me_4Si) 12.01 (1 H, br, NH-2), 8.67 (1 H, br s, OH py), 8.51 (2 H, s, py CHN + NH-4), 8.18 (1 H, s, py), 5.28 (1 H, t, OH), 4.75 (2 H, s, py CH_2O), 2.59 (2 H, s, CH_2), 1.74 (3 H, s, CH_3 py) and 1.14 (3 H, t, CH_3 CH_3CH_2N). *m/z* (EI) 267.8 ($M^+ = HCl·C_{11}H_{16}N_4O_2S$ requires 268), 165 (80%), 149 (42), 120 (9), 103 (14), 88 (10) and 60 (23).

$[Fe(Hthpy)_2](SO_4)_{1/2}·3.5H_2O$ 1. To a methanolic slurry of pyridoxalthiosemicarbazone hydrochloride, H_2thpy·HCl (0.553 g, 2 mmol) on constant stirring, was added a solution of $Fe_2(SO_4)_3·5H_2O$ (0.49 g; 1 mmol) in 20 mL of methanol. The resulting brown solution was stirred and heated mildly up to 40 °C for about half an hour before being allowed to stand at room temperature for 2 d. The dark brown microcrystals (0.289 g, 44.7%) were isolated by filtration, washed with methanol and diethylether, and dried in a well ventilated space for 24 h. Mp > 280 °C (from MeOH). (Found: C 33.46, H 4.63, N 16.99, S 12.51. Calcd for $C_{18}H_{29}FeN_8O_{9.5}S_{2.5}$: C 33.49, H 4.53, N 17.36, S 12.42%). The complex is readily soluble in methanol and sparingly soluble in water. ν_{max} (KBr)/cm^{-1} 1612 (CN), 1577 (py), 1381 (OH), 1247 (NN) and 1206, 1130, 998 and 605 (SO_4).

$[Fe(Hthpy)_2]NO_3·3H_2O$ 2. To a water slurry of recrystallized pyridoxalthiosemicarbazone monohydrate, H_2thpy·H_2O (2.68 g; 10.37 mmol) on constant stirring, was added a solution of $Fe(NO_3)_3·9H_2O$ (2.09 g; 5.19 mmol) in 20 mL of water resulting in a dark red solution. The final mixture was stirred and heated mildly up to 40 °C for about 15 min, before allowed to stand at room temperature for five days. The dark red microcrystals (2.10 g, 62.3%) were isolated by filtration, washed with methanol and diethylether, and dried in a well ventilated space for 24 h. Mp > 280 °C (from H_2O). (Found: C 32.91, H 4.27, N 19.37, S 10.06. Calcd for $C_{18}H_{28}$ $FeN_9O_{10}S_2$: C 33.24, H 4.34, N 19.38, S 9.86%). The complex is readily soluble in methanol and sparingly soluble in water. ν_{max} (KBr)/cm^{-1} 3457 (NH), 2895 (CH), 1620 (CN), 1464 (py), 1383 (NO_3), 1318 (OH), 1250 (NN) 1029 (CS) and 618 (NO_3).

$[Fe(H_2mthpy)_2](CH_3C_6H_4SO_3)_3·CH_3CH_2OH$ 3. To an ethanolic slurry of recrystallized pyridoxal-4-methylthiosemicarbazone monohydrate, H_2mthpy·H_2O (1.41 g, 5.19 mmol) on constant stirring, was added a solution of $Fe(CH_3C_6H_4SO_3)_3·6H_2O$ (1.76 g; 2.59 mmol) in 30 mL of ethanol resulting in a dark brown solution. The final mixture was stirred and heated mildly up to 40 °C for about 20 min and allowed to stand at room temperature for at least one week. The dark brown microcrystals (0.95 g, 32.8%) were isolated by filtration, washed with ethanol and diethylether, and dried in a well ventilated space for 24 h. Mp > 280 °C (from EtOH). (Found: C 45.13, H 4.84, N 10.28, S 14.12. Calcd for $C_{43}H_{55}$ $FeN_8O_{14}S_5$: C 45.95, H 4.93, N 9.97, S 14.26%). The complex is readily soluble in water and sparingly soluble in methanol. ν_{max} (KBr)/cm^{-1} 1617 (CN), 1496 (py), 1382 (OH), 1210 (NN), 1168 and 1122 (SO_3), 1009 (CS) and 568 (SO_3).

$[Fe(Hethpy)(ethpy)]·8H_2O$ 4. A solution of $Fe(NO_3)_3·9H_2O$ (1.05 g; 2.59 mmol) in 20 mL of water, was added dropwise to a mixture of concentrated ammonia (40 mL) and pyridoxal-4-ethylthiosemicarbazone hydrochloride, H_2ethpy·HCl (1.58 g; 5.19 mmol) in 40 mL of water on constant stirring. The resulting dark green solution was stirred and heated mildly up to 40 °C for about 10 min whereafter approximately 3 g of NH_4Cl salt was added. The final solution was stirred for 10 min and allowed to stand at room temperature for a period of one week. The dark green microcrystals (1.02 g, 53.6%) were isolated by filtration, washed with water and dried in a well ventilated space for 24 h. Mp > 280 °C (from H_2O). (Found: C 35.94, H 5.79, N 15.00, S 8.90. Calcd for $C_{22}H_{45}$ $FeN_8O_{12}S_2$: C 36.02, H 6.18, N 15.27, S 8.74%). The complex is soluble in DMSO, DMF, pyridine, and concentrated acidic and basic media. ν_{max} (KBr)/cm^{-1} 1636 (CN), 1543 (py), 1364 (OH), 1261 (NN), 1252.0 (w), 1206.9 (m), 1169.7 (m) and 1028 (CS).

Acknowledgements

The authors thank COST Action D35 "From Molecules to Molecular Devices: Control of Electronic, Photonic, Magnetic and Spintronic Behaviour" for the travel grant, Mr Lionel Rechignat and Mr Jean François Meunier from LCC-CNRS Toulouse for performing the EPR and the ^{57}Fe Mössbauer measurements, respectively.

References

1 (*a*) M. J. M. Campbell, *Coord. Chem. Rev.*, 1975, **15**, 279; (*b*) S. B. Padhye and G. Kauffman, *Coord. Chem. Rev.*, 1985, **63**, 127.
2 D. X. West, S. B. Padhye and P. B. Sonawane, *Struct. Bonding (Berlin, Ger.)*, 1991, **76**, 1.
3 D. X. West, A. E. Liberta, S. B. Padhye, R. C. Chikate, P. B. Sonawane, A. S. Kumbhar and R. G. Yerande, *Coord. Chem. Rev.*, 1993, **123**, 49.
4 J. S. Casas, M. S. Garcia-Tasende and J. Sordo, *Coord. Chem. Rev.*, 2000, **209**, 197.
5 D. R. Smith, *Coord. Chem. Rev.*, 1997, **164**, 575.
6 A. G. Quiroga and C. N. Ranninger, *Coord. Chem. Rev.*, 2004, **248**, 119.
7 D. L. Klayman, J. P. Scovill, J. F. Bartosevich and C. J. Mason, *J. Med. Chem.*, 1979, **22**, 1367.
8 C. Shipman, Jr., S. H. Smith, J. C. Drach and D. L. Klayman, *Antiviral Res.*, 1986, **6**, 197.
9 (*a*) V. V. Zelentsov, *Russ. J. Coord. Chem.*, 2003, **29**, 425; (*b*) V. V. Zelentsov, *Russ. J. Coord. Chem.*, 1992, **18**, 787; (*c*) V. V. Zelentsov, *Sov. Sci. Rev., B. Chem.*, 1987, **10**, 485; (*d*) V. A. Kogan, V. V. Zelentsov, G. M. Larin and V. V. Lukov, *Kompleksy perekhodnykh metallov s gidrazonami: Fiziko-khimicheskie svoistva i stroenie (Complexes of Transition Metals with Hydrazones: Physiochemical Properties and Structure)*, Moscow, Nauka, 1990, p 85.
10 P. J. van Koningsbruggen, Y. Maeda and H. Oshio, *Top. Curr. Chem.*, 2004, **233**, 259.
11 V. M. Leovac, V. S. Jevtovic, L. S. Jovanovic and G. A. Bogdanovic, *J. Serb. Chem. Soc.*, 2005, **70**, 393.
12 L. S. Jovanovic, V. S. Jevtovic, V. M. Leovac and L. J. Bjelica, *J. Serb. Chem. Soc.*, 2005, **70**, 187.
13 (*a*) M. Mohan, P. H. Madhuranath, A. Kumar, M. Kumar and N. K. Jha, *Inorg. Chem.*, 1989, **28**, 96; (*b*) N. S. Gupta, M. Mohan, N. K. Jha and W. E. Antholine, *Inorg. Chim. Acta*, 1991, **184**, 13.
14 J. R. Sams and T. B. Tsin, *J. Chem. Soc., Dalton Trans.*, 1976, 488.
15 J. R. Sams and T. B. Tsin, *Inorg. Chem.*, 1976, **15**, 1544.
16 A. T. Baker and H. A. Goodwin, *Aust. J. Chem.*, 1977, **30**, 771.
17 R. Boča, P. Baran, L. Dlháň, H. Fuess, W. Haase, F. Renz, W. Linert, I. Svoboda and R. Werner, *Inorg. Chim. Acta*, 1997, **260**, 129.
18 Y. Ikuta, M. Ooidemizu, Y. Yamahata, M. Yamada, S. Osa, N. Matsumoto, S. Iilima, Y. Sunatsuki, M. Kojima, F. Dahan and J.-P. Tuchagues, *Inorg. Chem.*, 2003, **42**, 7001.
19 M. Belicchi Ferrari, G. Fava Gasparri, E. Leporati, C. Pelizzi, P. Tarasconi and G. Tosi, *J. Chem. Soc., Dalton Trans.*, 1986, 2455.
20 E. W. Yemeli Tido, E. J. M. Vertelman, A. Meetsma and P. J. van Koningsbruggen, *Inorg. Chim. Acta*, 2007, **360**, 3896.
21 M. Belicchi Ferrari, F. Bisceglie, E. Leporati, G. Pelosi and P. Tarasconi, *Bull. Chem. Soc. Jpn.*, 2002, **75**, 781.
22 U. Abram, K. Ortner, R. Gust and K. Sommer, *J. Chem. Soc., Dalton Trans.*, 2000, 735.
23 E. W. Yemeli Tido, G. O. R. Alberda van Ekenstein, A. Meetsma and P. J. van Koningsbruggen, *Inorg. Chem.*, 2008, **47**, 143.
24 M. Belicchi Ferrari, G. G. Fava, M. Lanfranchi, C. Pelizzi and P. Tarasconi, *J. Chem. Soc., Dalton Trans.*, 1991, 1951.
25 M. Belicchi Ferrari, G. G. Fava, G. Pelosi, M. C. Rodriguez-Argüelles and P. Tarasconi, *J. Chem. Soc., Dalton Trans.*, 1995, 3035.
26 M. Belicchi Ferrari, F. Bisceglie, G. Pelosi, P. Tarasconi, R. Albertini, P. P. Dall'Aglio, S. Pinelli, A. Bergamo and G. Sava, *J. Inorg. Biochem.*, 2004, **98**, 301.
27 M. Belicchi Ferrari, G. Gasparri Fava, C. Pelizzi, P. Tarasconi and G. Tosi, *J. Chem. Soc., Dalton Trans.*, 1987, 227.
28 V. S. Jevtovic, L. S. Jovanovic, V. M. Leovac and L. J. Bjelica, *J. Serb. Chem. Soc.*, 2003, **68**, 929.
29 Z. Berkovitch-Yellin and L. Leiserowitz, *Acta Crystallogr., Sect. B: Struct. Sci.*, 1984, **40**, 159–165.
30 Th. Steiner, *Crystallogr. Rev.*, 1996, **6**, 1–57.
31 G. A. Jeffrey, M. Maluszynska and J. Mitra, *Int. J. Biol. Macromol.*, 1985, **7**, 336–348.
32 V. V. Zelentsov, in *Advances in Inorganic Chemistry*, ed. V. I. Spitsyn, MIR Publishers, 1983, p. 122.
33 (*a*) M. Nihei, T. Shiga, Y. Maeda and H. Oshio, *Coord. Chem. Rev.*, 2007, **251**, 2606; (*b*) H. Oshio, Y. Maeda and Y. Takashima, *Inorg. Chem.*, 1983, **22**, 2684; (*c*) R. M. Golding, *Mol. Phys.*, 1967, **12**, 13.
34 B. J. Kennedy, K. S. Murray, P. R. Zwack, H. Homborg and W. Kalz, *Inorg. Chem.*, 1986, **25**, 2539.
35 (*a*) M. D. Timken, D. N. Hendrickson and E. Sinn, *Inorg. Chem.*, 1985, **24**, 3947; (*b*) M. S. Shongwe, B. A. Al-Rashdi, H. Adams, M. J. Morris, M. Mikuriya and G. R. Hearne, *Inorg. Chem.*, 2007, **46**, 9558.
36 S. Hayami, Z. Z. Gu, H. Yoshiki, A. Fujishima and O. Sato, *J. Am. Chem. Soc.*, 2001, **123**, 11644.
37 R. Hogg and R. G. Wilkins, *J. Chem. Soc.*, 1962, 341.
38 R. N. Sylva and H. A. Goodwin, *Aust. J. Chem.*, 1967, **20**, 479.
39 (*a*) G. A. Renovitch and W. A. Baker, *J. Am. Chem. Soc.*, 1967, **89**, 6377; (*b*) M. Sorai, J. Ensling and P. Gütlich, *Chem. Phys.*, 1976, **18**, 199; (*c*) H. Spiering, E. Meissner, H. Köppen, E. W. Müller and P. Gütlich, *Chem. Phys.*, 1982, **68**, 65.
40 (*a*) M. C. Giménez-López, M. Clemente-León, E. Coronado, F. M. Romero, S. Shova and J.-P. Tuchages, *Eur. J. Inorg. Chem.*, 2005, 2783–2787; (*b*) M. Clemente-León, E. Coronado, M. C. Giménez-López and F. M. Romero, *Inorg. Chem.*, 2007, **46**, 11266.
41 A. M. Greenaway and E. Sinn, *J. Am. Chem. Soc.*, 1978, **100**, 8080.
42 K. H. Sugiyarto, D. C. Craig, A. D. Rae and H. A. Goodwin, *Aust. J. Chem.*, 1993, **46**, 1269.
43 (*a*) Y. Tanabe and S. Sugano, *J. Phys. Soc. Jpn.*, 1954, **9**, 753; (*b*) Y. Tanabe and S. Sugano, *J. Phys. Soc. Jpn.*, 1954, **9**, 766.
44 F. Varret, *International Conference on Mössbauer Effects Applications, Indian National Science Academy*, New Delhi, Jaipur, India, 1981.
45 *Bruker, SMART, SAINTPLUS and XPREP, Area Detector Control and integration Software, Smart Apex Software Reference Manuals*, Bruker Analytical X-ray instruments Inc., Madison, Wisconsin, USA, 2000.
46 G. M. Sheldrick, *SADBAS version 2.03, Multi-scan absorption correction program*, University of Göttingen, Germany, 2001.
47 M. C. Burla, R. Caliandro, M. Camalli, B. Carrozzini, G. L. Cascarano, L. De Caro, C. Giacovazzo, G. Polidori and R. Spagna, SIR2004. An improved tool for crystal structure determination and refinement, *J. Appl. Crystallogr.*, 2005, **38**, 381–388.
48 P. T. Beurskens, G. Beurskens, R. de Gelder, S. García-Granda, R. O. Gould, R. Israël and J. M. M. Smits, *The DIRDIF-99 program system*, Crystallography Laboratory, University of Nijmegen, The Netherlands, 1999.
49 P. T. Beurskens, G. Beurskens, R. GelderJ. M. M. de Smits, S. García-Granda, and R. O. Gould, *The DIRDIF-07 program system*, Crystallography Laboratory, University of Nijmegen, The Netherlands, 2007.
50 *International Tables for Crystallography*, ed. A. J. C. Wilson, vol. C, Kluwer Academic Publishers, Dordrecht, The Netherlands, 1992.
51 T. Hahn, ed. *International Tables for Crystallography*, Vol. A, Space-group symmetry, Kluwer Academic Publishers, Dordrecht, The Netherlands, 1983.
52 G. M. Sheldrick, *SHELXL-97, Program for the refinement of crystal structures*, University of Göttingen, Germany, 1997.
53 A. Meetsma, *PLUTO, Molecular graphics program, Version of March 2006*, University of Groningen, The Netherlands, 2006.
54 A. Meetsma, *PLUTO, Molecular graphics program. Version of March 2008*, University of Groningen, The Netherlands, 2008.
55 (*a*) A. L. Spek, *PLATON, Program for the automated analysis of molecular geometry (A Multipurpose Crystallographic Tool), Version of February 2006*, University of Utrecht, The Netherlands, 2006; (*b*) A. L. Spek, *J. Appl. Crystallogr.*, 2003, **36**, 7.
56 (*a*) A. L. Spek, *PLATON. Program for the automated analysis of molecular geometry (A Multipurpose Crystallographic Tool)*, Version of March 2008, University of Utrecht, The Netherlands, 2008.